GSA DATA REPOSITORY 2013057

SUPPLEMENTARY MATERIAL

Aseismic plate boundary in the Indo-Burmese wedge, northwest Sunda Arc

Vineet K Gahalaut[1*], Bhaskar Kundu[1], Sunil Singh Laishram[2], Joshi Catherine[1], Arun Kumar[2], M. Devchandra Singh[2], R.P.Tiwari[3], R.K. Chadha[1], S.K.Samanta[4], A Ambikapathy[1], P.Mahesh[1], Amit Bansal[1], M Narsaiah[1]

1 National Geophysical Research Institute (CSIR), Hyderabad, India
2 Department of Earth Sciences, Manipur University, Imphal, India
3 Department of Geology, Mizoram University, Aizwal, India
4 Department of Geological Sciences, Jadavpur University, Kolkata, India
* vkgahalaut@yahoo.com

MODELLING THE ASEISMIC SLIP USING ANSYS

The interseismic deformation and the effects of crustal faults were modeled with the finite element method (FEM) using the ANSYS® (http://www.ansys.com/) Academic Research software package v. 10.0. ANSYS employs the Newtonian-Raphson approach to solve nonlinear problems. In this method a load is subdivided into a series of increments applied over several steps. Before each solution the Newton-Raphson method evaluates the out-of-balance load vector, which is the difference between the restoring forces and the loads corresponding to the element stresses and the applied loads.

In our model, the CMF is considered as a steeply dipping fault which joins the plate boundary interface between the Indian plate and Burma sliver. We considered a 2 layer model in which the upper layer represents the IBW while the lower layer represents the Indian plate. The material in both the layers was considered to be perfectly elastic. On the basis of the seismicity data (EHB catalogue available at www.isc.ac.uk/ehbbulletin/, and Kundu and Gahalaut, 2012) and seismological studies related to receiver function (Mitra et al., 2005), the wedge thickness was considered as 25 km under the CMF. The friction on the CMF in the wedge (in the upper layer) was allowed to vary, while the plate boundary interface in layer 2 it was assumed as zero (actually it was considered as 0.05, to avoid singularity) to simulate the steady aseismic slip. The model has horizontal dimensions of 375 km (along the east west direction) x 200 km (along north south direction) and a depth extent of 45 km. The model is composed entirely of four-node tetrahedron solid structural elements, and consists of 94,039 elements with 19,114 active nodes. The mesh was refined at the frictional contact surface. All elements deform elastically and follow coulomb friction failure criterion. The force for the Coulomb friction is described as

$$F_f = \begin{cases} K \cdot u_t & : K \cdot u_t \le \mu \cdot F_n \text{ (sticking)}, \\ \mu \cdot F_n & : K \cdot u_t > \mu \cdot F_n \text{ (sliding)}, \end{cases}$$

where, u_t is the tangential displacements, μ is the friction coefficient and K is the stiffness coefficient.

The model is subjected to gravity, which compressed the model and established an initial stress state. The bottom of the model was constrained to zero displacement in the vertical direction, and the model sides were not permitted to move vertically (fixed in Y direction). All other nodes were given 2 DOF, i.e., in X and Z direction. Thus, the velocity of the western part (i.e., representing Indian plate, 300 km west of the CMF) of the model is fixed to zero. We imposed a velocity of 18.6 mm/year towards N222° on the eastern edge of the model which corresponds to the site velocity at MORE, the easternmost site of our network located at the eastern margin of the wedge (75 km east of CMF). The free surface is fully deformable. All velocity constraints are imposed on the model edges as described above and no constraints are imposed on elements within the model. Pore fluid pressure was assumed to be hydrostatic. Results were considered along an east west profile on the surface passing through the centre. The model is shown in Fig.DR7.

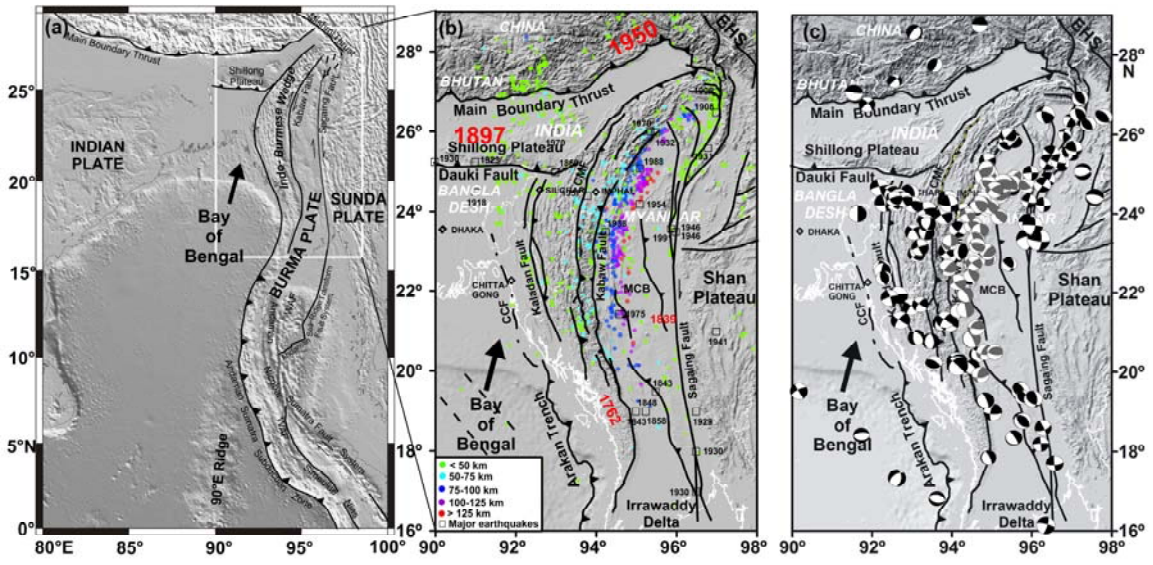

Figure DR1: General tectonics of the Sunda arc. Arrow in (a) shows the India Sunda relative motion (36 mm/year). Seismicity and earthquake focal mechanisms are shown in (b) and (c). All historical great and major earthquakes are also shown. CCF- Chittagong Coastal fault, MCB- Myanmar Central Basin, CMF- Churachandpur Mao Fault, EHS- Eastern Himalayan Syntaxis.

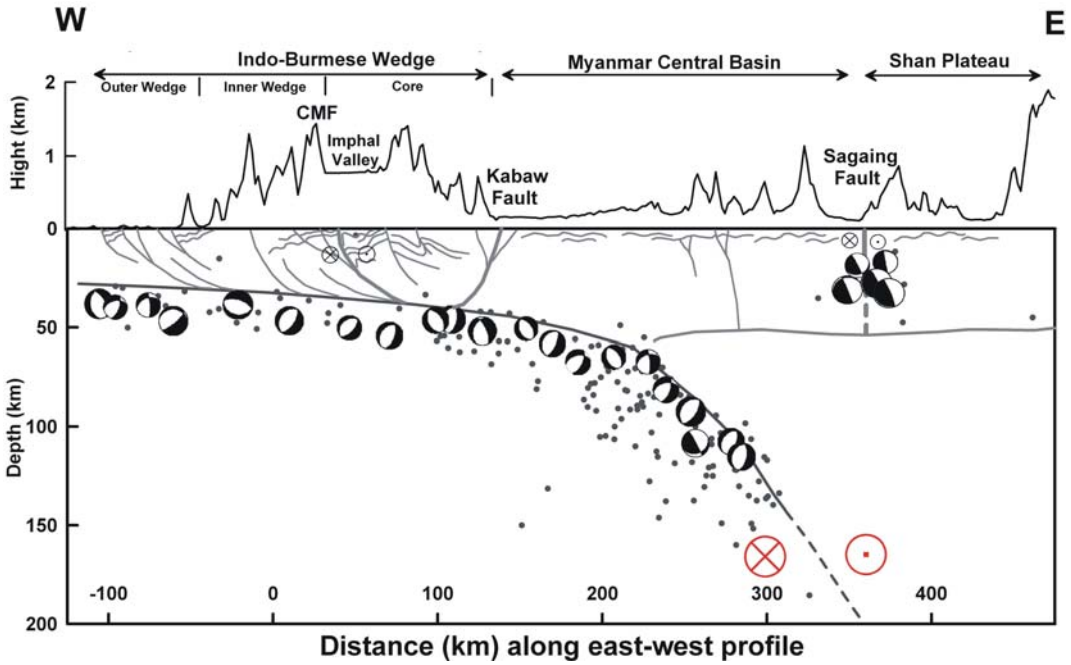

Figure DR2: A west to east vertical cross section across the Indo Burmese wedge and Sagaing fault showing seismicity and focal mechanisms of earthquakes (Kundu and Gahalaut, 2012). Geometry of the faults is schematic.

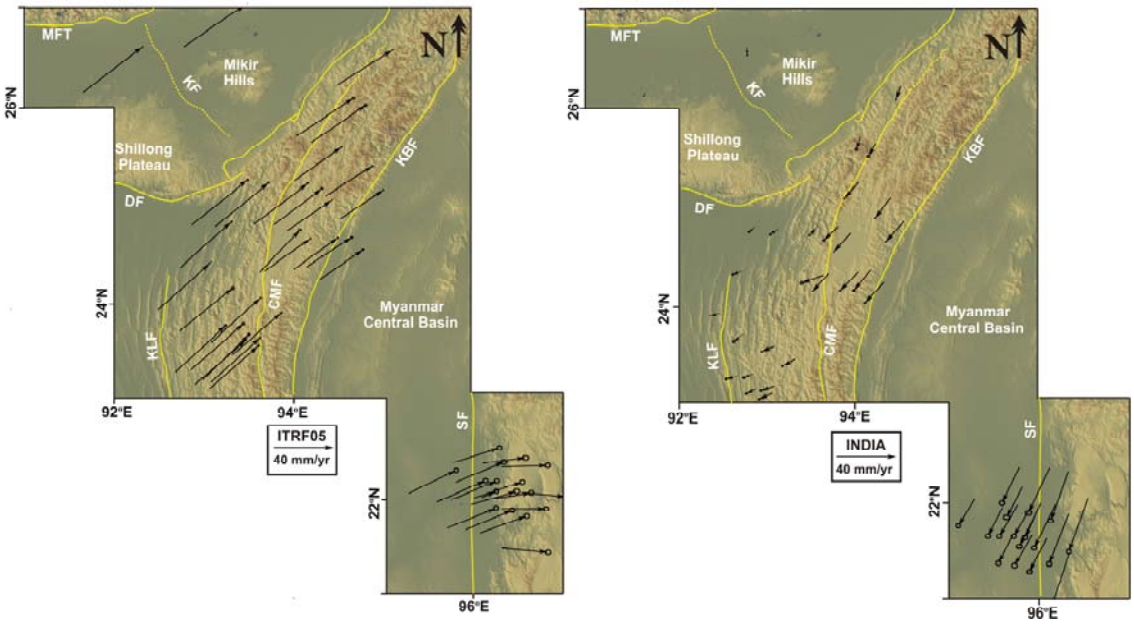

Figure DR3: Velocity of sites in the IBW and Sagaing Fault (Vigny et al., 2003; Maurin et al., 2010) in ITRF2005 and Indian reference frame. MFT-Main Frontal Thrust, KF-Kopili fault, DF- Dauki fault, KLF- Kaladan fault, CMF- Churachandpur Mao fault, KBF- Kabaw fault, SF- Sagaing fault.

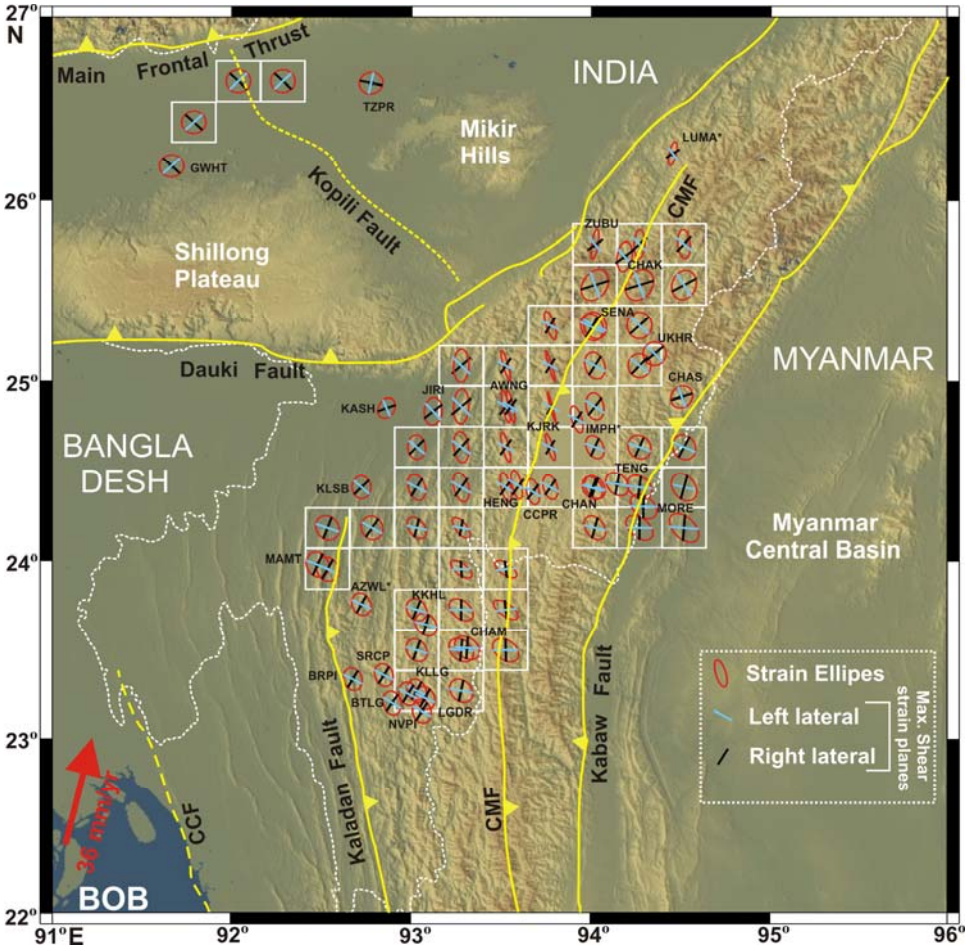

Figure DR4: The horizontal 2D strain rate principal axes and their directions on a specified grid. The analysis is done using SSPX computer program (Cardozo et al., 2008), by applying the distance weighted approach on a regularly spaced grid to estimate the strain using all the GPS sites in the region. Note high strain rate across the CMF in the central part. Due to lack of GPS sites, east of the CMF in the southern part, the strain rate is not well constrained.

Figure DR5: A mosaic of field photographs of the CMF.

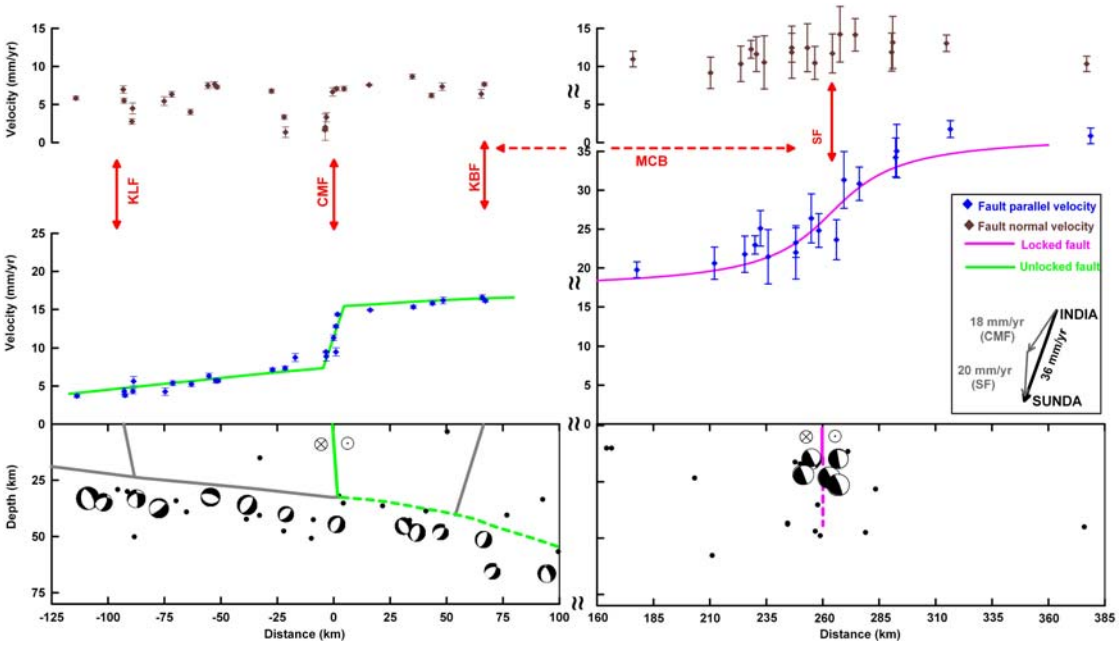

Figure DR6: Fault parallel and fault normal motion along east west profile in the IBW (left panels) and Sagaing fault (right panels) region. There is no apparent jump in the fault normal velocities across the two tectonic features, implying that there is no subduction along this margin. The jump in fault parallel velocity in the IBW and Sagaing fault is simulated with predominantly aseismic motion on the CMF and seismogenic slip of 20.3±3 mm/year along the Sagaing fault (Vigny et al., 2003; Maurin et al., 2010). The inset shows the partition of the India Sunda motion along the CMF in IBW and Sagaing fault. Lower panel shows the geometry of the faults in the IBW and Sagaing fault. Dashed portion of the fault at depth (or plate boundary interface) denote stable sliding in both the lower panels.

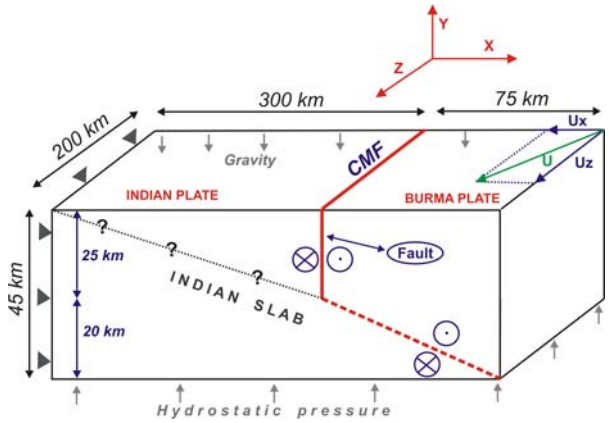

Figure DR7: A generalized model of the simulation. U corresponds to the site velocity of the easternmost GPS site, MORE. The dimensions are representative and are not to the scale.

Table DR1: Estimated site velocity in ITRF2005 (Altamimi, 2007) and Indian reference frame (Banerjee et al., 2008). Sites marked with an asterisk represent permanent GPS sites.

GPS sites	Longitude (°E)	Latitude (°N)	ITRF2005		Indian reference frame		E-error (mm/yr)	N-error (mm/yr)
			East (mm/yr)	North (mm/yr)	East (mm/yr)	North (mm/yr)		
CHAS	94.508	24.868	29.61	19.84	-11.87	-13.52	0.19	0.17
LUMA*	94.475	26.220	37.80	24.31	-3.29	-9.05	0.14	0.12
UKHR	94.360	25.109	31.20	19.73	-10.18	-13.64	0.26	0.23
MORE	94.290	24.258	29.10	19.56	-12.50	-13.81	0.40	0.34
CHAK	94.199	25.652	36.30	24.59	-4.88	-8.78	0.60	0.54
TENG	94.146	24.384	30.26	19.65	-11.27	-13.73	0.49	0.43
ZUBU	94.035	25.718	38.12	25.02	-3.00	-8.36	0.62	0.54
SENA	94.013	25.261	31.46	22.78	-9.79	-10.60	0.21	0.18
CHAN	94.009	24.363	29.28	20.80	-12.23	-12.59	0.25	0.22
IMPH*	93.925	24.749	30.23	20.93	-11.15	-12.46	0.10	0.09
KJRK	93.785	24.817	31.92	24.17	-9.40	-9.22	0.41	0.37
CCPR	93.679	24.344	30.75	21.41	-10.68	-11.99	0.19	0.16
HENG	93.624	24.331	27.06	28.03	-14.36	-5.37	0.70	0.62
AWNG	93.559	24.821	36.09	27.17	-5.18	-6.23	0.30	0.26
CHAM	93.313	23.480	33.16	28.26	-8.43	-5.15	0.25	0.22
JIRI	93.128	24.796	35.92	29.38	-5.25	-4.04	0.34	0.30
KKHL	93.087	23.611	32.95	29.81	-8.55	-3.61	0.23	0.19
LGDR	93.082	23.202	32.81	29.88	-8.80	-3.54	0.36	0.30
NVPI	93.064	23.129	32.78	29.22	-8.84	-4.20	0.40	0.34
BTLG	92.901	23.175	34.09	29.86	-7.48	-3.57	0.37	0.32
KASH	92.869	24.814	37.29	29.97	-3.81	-3.46	0.36	0.32
SRCP	92.856	23.329	35.15	30.71	-6.37	-2.72	0.58	0.49
TZPR*	92.780	26.618	40.91	27.69	0.38	-5.74	0.11	0.10
AZWL*	92.732	23.724	35.65	29.13	-5.73	-4.30	0.73	0.61
KLSB	92.731	24.371	34.89	31.19	-6.31	-2.24	0.27	0.24
BRPI	92.685	23.306	33.68	31.05	-7.81	-2.39	0.48	0.42
MAMT	92.490	23.943	34.65	31.38	-6.61	-2.06	0.24	0.20
GWHT*	91.661	26.153	39.67	30.95	-0.72	-2.51	0.14	0.12

REFERENCES CITED

Altamimi, Z. X. Collilieux, J. Legrand, B. Garayt, and C. Boucher, ITRF2005: 2007, A new release of the International Terrestrial Reference Frame based on time series of station positions and Earth Orientation Parameters, J. Geophys. Res., v.112, B09401, doi:10.1029/2007JB004949.

Banerjee, P., Bürgmann, R., Nagarajan, B., and Apel, E., 2008, Intraplate deformation of the Indian subcontinent: Geophys.Res. Lett., v.35, doi:10.1029/2008GL035468.

Cardozo, N. and R.W. Allmendinger, SSPX: 2008, A program to compute strain from displacement/velocity data, Comput. Geosci., v.35, p.1343–1357.

Jade, S., M. S. M. Vijayan, S. S. Gupta, P. D. Kumar, V. K. Gaur and S. Arumugam, 2007, Effect of the M 9.3 Sumatra–Andaman islands earthquake of 26 December 2004 at several permanent and campaign GPS stations in the Indian continent, International Journal of Remote Sensing, v.28, p.3045–3054.

Kundu, B., and Gahalaut, V.K., 2012, Earthquake occurrence process in the Indo-Burmese wedge and Sagaing fault region, Tectonophysics, v.524, p.135-146.

Maurin, T., Frederic Masson, Claude Rangin, U Than Min, and Philippe Collard, 2010, First global positioning system results in northern Myanmar: Constant and localized slip rate along the Sagaing fault, Geology, v.38, p.591-594.

Mitra, S., Priestley, K., Bhattacharyya, A., Gaur, V.K. 2005, Crustal structure and earthquake focal depths beneath northeastern India and South Tibet. Geophysical Journal International v.160, p.227–248.

Vigny, C., A. Socquet, C. Rangin, N. Chamot-Rooke, M. Pubellier, M. Bouin, G. Bertrand, and M. Becker 2003. Present-day crustal deformation around Sagaing fault, Myanmar, J. Geophys. Res., v.108, 2533, doi:10.1029/2002JB001999.